Microdosimetric spectra simulated with MCNP6.1 with INCL4/ABLA model for kerma and mean quality factor assessment, for neutrons between 100 keV to 19 MeV

Rodolphe Antoni, Laurent Bourgois

Version of Record: https://www.sciencedirect.com/science/article/pii/S1350448719304755
Manuscript_60088094eb900a0647e708bfcfad1457

Microdosimetric Spectra simulated with MCNP6.1 with INCL4/ABLA model for Kerma and mean quality factor assessment, for neutrons between 100 keV to 19 MeV

R. Antoni (1)‡, L. Bourgois (2)
(1) CEA, DEN, CAD, (2) CEA,DAM, DIF
‡ corresponding author rodolphe.antoni@cea.fr

Abstract : From the application of the microdosimetric approach in dosimetry, the standard TEPC, i.e., Rossi-type detector, was found to be a well-suited device to measure "first collision" neutron kerma and develop lineal energy spectra for incident neutrons. Subsequently, several attempts were carried out to assess the ambient dose equivalent for neutrons, with a mixed outcome, through the evaluation of the mean quality factor. The ICRU report 63, released in 2000, has officially recognized a good agreement between theoretical Kerma factor and value measured with standard TEPCs for neutron energies ranging over 5 to 66 MeV. As a follow-up, benchmark with simulated results for Kerma calculation and lineal energy spectra concluded to a satisfactory agreement for Monte-Carlo transport codes such as FLUKA or GEANT4. Nevertheless, previous studies have highlighted major discrepancies with MCNP results for energy above the capture threshold, mainly stemming from the weakness of the alpha release. This paper emphasizes the improvement of the kerma factor calculation as well as the development of lineal energy spectra from a standard A150 plastic-wall TEPC with MCNP6.1. The shortcomings of the alpha release are overcome using INCL4 /ABLA implementation instead of the default model for the Intra-nuclear cascade. This new approach lead to lineal energy spectra overlapping those from experiments. In addition, the neutron kerma is evaluated with a mean relative deviation not exceeding 5% of the ICRU standard values, for mono-energies from 100 keV to 19 MeV. This new approach is also relevant for usual neutron sources as AmBe and ^{252}Cf with a maximum deviation of roughly 6%. Nevertheless, major discrepancies remain for evaluation of the quality factor at the depth of 10 mm inside de ICRU sphere, with a mean relative deviation of 17%. However, this finding is consistent with discrepancies in literature As regards the prospects, satisfactory results on lineal energy spectra and kerma evaluation henceforth offers the possibility to simulate microdosimetric spectra and determine neutron kerma for energies higher than a hundred keV up to twenty MeV.

Key words: microdosimetry, MCNP6.1, neutron kerma factor, lineal energy spectra, Tissue-Equivalent Proportionnal Counter, quality factor, ambient dose equivalent

I - Introduction

The Tissue-Equivalent Proportional Counter (TEPC) is found to be an accurate detector to develop microdosimetric spectra for charged and non-charged particles [1]. TEPCs are also suited well for measurement of absorbed dose and assessment of dose equivalent in various contexts of radiation protection [2]. In case of neutrons, for standard Rossi-type TEPCs, heavy charged particles set in motion in the surrounding wall of the cavity (recoil protons, alpha and recoil heavy ions) are responsible for ionizations in the low gas pressure cavity that afford the measurement of "single collision" Kerma with the collection of the entire charge. Furthermore, for each secondary particle, ionizations may be separately detected, i.e. single events detection. The charge from each single event is directly proportional to the energy imparted in the sensitive volume and therefore to the lineal energy. The lineal energy distribution may yield the mean quality factor for mono-energetic neutrons and quasi-monoenergetic neutrons [3],[4]. Then both quantities allow the assessment of ambient dose equivalent in a restricted energy range.

For a few years, the studies on the feasibility of micro-pattern (small-sized) gaseous detectors, including TEPCs have led to some useful developments [5]. Recent comparison between experiment and GEANT 4 simulation concluded that a THGEM-based microdosimeter of 1 μm tissue-equivalent reliably determined the dose-equivalent value of each neutron field with energy spectrum lying between 20 keV and 14 MeV, along with the energy spectrum of ^{241}Am-Be neutrons with a deviation of no more 20% [5].
Monte-Carlo code MCNP6.1 [7] is able to simulate the lineal energy spectra for TEPCs with separate contributions for secondary's charged particles. Nevertheless, the comparison with standard TEPCs measurements as well as results from GEANT 4 and FLUKA simulations could indicate major discrepancies for both the neutron kerma and the mean quality factor mainly traced back to shortcomings in the amount of secondary alpha particles released in (n,α) captures [8]. This paper emphasizes the better assessment of both dosimetric quantities from standard TEPC with MCNP6.1. This improvement is enabled through the overcoming of the lack of alpha particles released using INCL4 [9]/ABLA [28] [29] implementation for the Intra-nuclear cascade for neutron energy above the capture threshold. In what follows, an evaluation with the new MCNP approach is achieved for energies ranging from 100 keV to 20 MeV for a standard TEPC, i.e., Rossi-type, with a A150 tissue-equivalent plastic wall based on the detector used in Menzel & al. experiment [3]. The simulated results are compared to values from Caswell & al. [10] for kerma factors, Leuthold & al. [12] for mean quality factor and ICRP 74 [23] values for fluence-to-ambient dose equivalent factors.

II - Measurement and theoretical approaches for kerma factor determination

The ICRU report 63 [11] provides results of Kerma factors for A-150 plastic measured by integral methods, derived from different contributors and for neutron energies from 5 to 66 MeV neutrons. Between the latter, Menzel & al. [3] have measured neutron kerma factors with a low-pressure Rossi type TEPC (also so-called LPPC) for mono-energetic neutrons ranging over 13.9 to 19 MeV. This detector is herein considered and simulated with MCNP6.1. It is designed with a spherical Proportional counter of $1.27\ cm$ inner diameter for which the outer shell is composed of A150 tissue-equivalent plastic mainly made of C (77.5% by weight), H (10.1%), O (5.2%), N (3.5%), with a wall thickness of $2.54\ mm$. It should be noted that the wall is thick enough to maintain charged particle equilibrium during neutron irradiation. The inner cavity is filled with a low-pressure methane based tissue-equivalent gas mixture ($7.4\ kPa$) with density of $1.064 \times 10^{-3} g.cm^{-3}$ TPN. Therefore, these parameters allow for a mass thickness of $10^{-4} g.cm^{-2}$ and an tissue-equivalent thickness of $1\ \mu m$ for a $1\ g.cm^{-3}$ tissue density that corresponds to the order of magnitude of cellular structure. When neutrons interact with the counter wall, reactions like $(n,n), (n,p), (n,t), (n,\alpha)$ occur … then the bulk of secondary's charged particles, including recoil heavy ions (C, O and N) pass by the gas cavity, undergoing many ionizations throughout the path. The figure 1 shows a schematic layout of the Rossi type TEPC used.

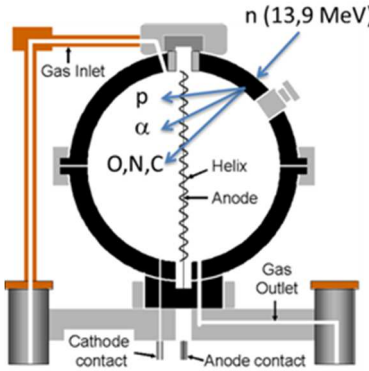

Figure 1 : Sectional view of a schematic layout of the Rossi type TEPC for lineal-energy spectra and kerma factor calculation (adapted from Oak Ridge Associated Universities)

For a detector operating in proportional counter mode, the collected charge q from ionizations is directly connected to the imparted energy ε for each single event. A broad lineal energy spectrum can then be draw up since the corresponding lineal energy for each single event is given by ratio of imparted energy by the mean chord $y = \varepsilon/\bar{l}$; the mean chord is here given by $\bar{l} = 2d/3$ where d stands for the equivalent tissue diameter of 1 µm. Then the charge distribution $qn(q)$ at the reference point closely matches to microdosimetric spectra $yd(y)$. The integration over the entire $qn(q)$ distribution lead to the entire charge Q. The cavity fulfills the Bragg-Gray conditions for secondary's charged particles set in motion and then the fluence-to-neutron Kerma conversion coefficient, i.e., Kerma factor, against the current i is given by [3]:

$$\left(\frac{K}{\Phi}\right)_{E_n} = 6.38 \times 10^{-4} \frac{i}{\rho \pi d^2 q_\alpha \dot{\Phi}} \frac{\left(\overline{W_g}\right)_n}{\left(\overline{W_g}\right)_\alpha} \left(\frac{\bar{S}}{\rho}\right)_g^W \left(\frac{\Delta\varepsilon_\alpha}{\bar{l}}\right) \qquad (eq.\ 1)$$

With :

- $\dot{\Phi}$, The neutron fluence rate at the reference point of the cavity,
- ρ, the cavity gas density,
- d, the inner cavity diameter,
- $\Delta\varepsilon_\alpha/\bar{l} = 1277\ MeV.g^{-1}$, the α stopping power in methane gas for an α released by an AmBe source [13],
- $q_\alpha = 4.86 \times 10^{-16} C$, the average charge produced by an α particle, estimated from $\Delta\varepsilon_\alpha/\bar{l}$,
- $\left(\overline{W_g}\right)_n/\left(\overline{W_g}\right)_\alpha = 1$,the ratio of mean ionizing energy in methane gas for neutron by α from AmBe,
- $(\bar{S}/\rho)_g^W = 1$, is the gas-to-wall absorbed dose conversion factor for secondary's particles set in motion in the counter wall.

The intensity i is corrected by a product of correction factors, which take account of ion recombination, leakage current, and polarity effects in counter... The standard kerma factors from ICRU report 63 rely on Caswell & al. work [10] and were calculated according to the theoretical approach detailed by Ritts & al., 1969 [14]. This factor, in $Gy.cm^2$, may be expressed as :

$$\left(\frac{K}{\Phi}\right)_{E_n} = 1.6 \times 10^{-10} \eta_A \sum_c \frac{w_c}{A_c} \sum_i \sigma_{c,i}(E_n)\, \bar{\varepsilon}_{c,i}(E_n) \qquad (eq.2)$$

With η_A the Avogadro number, w_c the weight fraction of the element c, A_c is the atomic mass of element c, $\sigma_{c,i}(E_n)$ is the microscopic cross section of reaction i for element c and $\bar{\varepsilon}_{c,i}(E_n)$ is the

average amount of energy transferred to kinetic energy of charged particles in a collision whose cross section is $\sigma_{c,i}$. All published expressions for $\bar{\varepsilon}_{c,i}(E_n)$, depending on reaction, are available in Ritts et al. [14].

III - Modeling the microdosimetric spectra, kerma factor and mean quality factor with MCNP.

Overall, the TEPC design modelled with MCNP6.1 is similar to the layout shown in figure 1 and with parameters detailed in the above section. The cavity irradiated by a free-field planar source of 13.9 MeV neutrons with a cross section of 1 cm radius. The composition of A150 plastic and tissue -equivalent methane derive from McConn Jr & al. [15]. The geometry as modelled in MCNP is displayed in fig. 2.

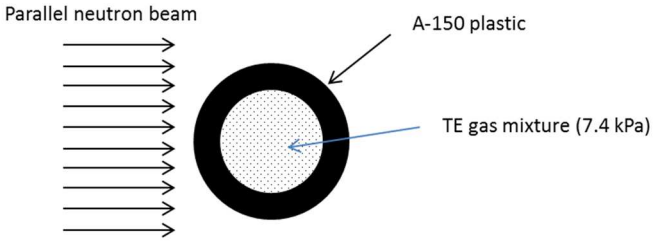

Fig. 2 : geometry in MCNP for the standard TEPC (not to scale)

The lineal energy distribution for each secondary heavy charged particles is estimated using a f6 tally type for energy deposition coupled to a pulse height tally F8 for each heavy charged particle specie [16]. An anticoincidence pulse height ft card, i.e, ft8 phl, is added to the f8 tally for counting single-event of imparted energy in gas due to specific nuclear reaction in the cavity wall. In addition, an energy spectra card, i.e., e8, enables the energy distribution of lineal energy counts in the gaz. For setting up this card, 185 logarithmic lineal energy bin are defined to ensure about 50 equal subdivisions per decade between 0.6 and 3030 keV.μm^{-1}. In what follows, we define both quantities ε_i and n_i respectively as the energy imparted in the cavity gas and the scored event in the lineal energy bin i, i.e., the f8 result in bin i,. The lineal energy of the bin i is given by the imparted energy divided by the mean chord length of 1 μm of tissue and multiplied by 10^3 for a MeV-to-keV conversion:$y_i = (1000/(2/3))\varepsilon_i = 1500\,\varepsilon_i$. For each y_i, the frequency distribution is given by $f(y_i) = n_i/\sum_i n_i$, with i up to 185, and normalized to unity for the whole y_i. This frequency distribution yields the mean frequency energy $\bar{y}_f$ (keV μm^{-1}) and the mean lineal energy $\bar{y}_D$ (keV μm^{-1}), calculated from MCNP results as the following equations 3 and 4.

$$\bar{y}_f = \int_0^\infty y f(y) dy \approx 1500 \frac{\sum_i \varepsilon_i n_i}{\sum_i n_i} \quad (eq.3)$$

$$\bar{y}_D = \frac{\int_0^\infty y^2 f(y) dy}{\bar{y}_f} \approx 1500 \frac{\sum_i \varepsilon_i^2 n_i}{\sum_i \varepsilon_i n_i} \quad (eq.4)$$

The first quantity, $\bar{y}_f$, relates the most likely lineal energy of counted events and the second, $\bar{y}_D$,the lineal-energy that contributes the most to the entire neutron kerma. These latest quantities are supposed to be linked to the mean quality factor [30]. In order to plot the microdosimetric spectra, the lineal energy distribution of absorbed dose $d(y)$ is defined as:

$$d(y) = \frac{yf(y)}{\bar{y}_f}$$

For the graphical representation, it is relevant to plot $d(y)$ in logarithmic scale:

$$d(y) = \frac{dD}{dy} \;\Rightarrow\; d(y) = \frac{dD}{d(\ln y)} \Leftrightarrow yd(y) = \frac{dD}{dy}$$

As a result, $yd(y)$ is the standard quantity for the y-axis while x-axis is linear. This distribution is also normalized to unity by integrating on the entire lineal energy range. From MCNP results, the $yd(y)$ distribution is calculated as follows:

$$\Leftrightarrow\; y_i d(y_i) = \frac{\varepsilon_i n_i}{\sum_i \varepsilon_i n_i}\left(\frac{1}{\ln(\varepsilon_i/\varepsilon_{i-1})}\right)$$

And the "single collision" kerma factor is calculated by eq.7:

$$\left(\frac{K}{\Phi}\right)_{E_n} = 1{,}6.10^{-13}\left(\frac{\bar{l}}{\Phi\rho V}\right)\sum_i y_i n_i = \frac{1{,}6.10^{-10}}{\Phi\rho V}\sum_i \varepsilon_i n_i$$

Where V and ρ stand for the volume and the density of the inner gas. The mean quality factor $\bar{Q}$ may be assessed with the lineal energy distribution of absorbed dose $d(y)$ by :

$$\bar{Q} = \frac{\int_0^\infty Q(y)d(y)dy}{\int_0^\infty d(y)dy}$$

By replacing $d(y)$ by $yf(y)/\bar{y}_f$, $\bar{Q}$ is calculated from MCNP results according to eq. 5 :

$$\bar{Q} \approx \frac{\sum_i Q(y_i)\, y_i f(y_i)}{\sum_i\, y_i f(y_i)} = \frac{\sum_i Q(y_i)\varepsilon_i n_i}{\sum_i \varepsilon_i n_i} \quad (eq.5)$$

Where $Q(y)$ vs. y is recommended by ICRU 40 [25] expressed as:

$$Q(y_i) = \frac{a}{y_i}\left[1 - exp(-by_i{}^2 - cy_i{}^3)\right] \quad (eq.6)$$

With following parameters: $a = 5510\ keV \cdot \mu m^{-1}$, $b = 5 \cdot 10^{-5}\ keV^{-2} \cdot \mu m^2$ and $c = 2 \cdot 10^{-7}\ keV^{-3} \cdot \mu m^3$. Finally, an estimator of the fluence-to-ambient dose equivalent $H^*(10)/\Phi$ can be defined with both previous dosimetric quantities, for a given energy, as following:

$$\left(\frac{\hat{H}}{\Phi}\right) = \left(\frac{K}{\Phi}\right)\bar{Q} \approx \left(\frac{D^*(10)}{\Phi}\right)Q^*(10) = \left(\frac{H^*(10)}{\Phi}\right)$$

Where $D^*(10)$ and $Q^*(10)$ are respectively the absorbed dose and the quality factor at the depth of 10 mm inside the ICRU sphere [23]. With very similar approach for calculation, Ali & al. [8] concluded that MCNPX code was not able to fully model the production and transport of alpha particles produced by captures due to the lack of an event generator to perform this modelling for energy upper than capture threshold [8]. Since the release of secondary alpha from (n,α) captures stems from the choice of physics model for intra-nuclear cascade INC, in the forthcoming analysis, evaluations are separately made with the default physics model (CEM03.03) - probably used in the Ali & al. evaluation [8] - and with the INCL4/ABLA model for the new proposed approach in this paper.

Computer time for running charged particle simulations in MCNP6 is significant. Each input deck was run using 7.10^8 histories to ensure a statistically accurate response. The tally converges and passes all 10 statistical checks.
The relative error was used to evaluate the deviation of different quantities (see table 2)

III.1 - Physical parameters for the default model

The transport mode runs with neutrons (n), protons (h), alpha (a) and heavy ions (#). Deuteron and triton are omitted because of sub-threshold: for the upper energy, i.e., 19 MeV, the contribution of deuteron bump represents only 0.4% of the total kerma factor [21]. The 7th parameter of the "phys:n" card and "phys:p" is set to 1 to ensure the generation and transport of recoil and (n,p) protons as well as recoil heavy ions. The second entry of the "phys:n" card, "emcnf", is set to 20 MeV and parameters wc1 = wc2 = 0 in the "cut" card for n, h, a and # to turn on analogue capture treatment below this energy. The libraries endf71x («.80c»), endf70prot («.70h») and tendl17 [17] are used respectively for neutrons protons and alpha transport. The 1st entry of the "cut:h, a, #" card is set to 1 keV to transport the whole particles above this cut-off energy. Furthermore, an "Act" card is added and set with "act fission=none nonfiss=a" to afford delayed alpha emission from simple multi-particle reaction activation events [7]. Special attention should be paid to the transport of charged particles in MCNP that is handled with a class I algorithm. The small size of the cavity requires setting the number of sub-steps to an appropriate value by the means of the "hstep" card. This card works the same way as "estep" card for electrons and the number of sub-steps is determined the same way. For this calculation, readers can refer to Antoni & Bourgois [26]

III.2 - Physical parameters for the INCL4/ABLA model

All previous parameters, for the default model, remain unchanged except for neutrons libraries that are replaced with model through the mix-and-match card. In order to improve the release of secondary alpha, the INCL4/ABLA model is turned on adding the LCA card with the 9th entry, "icem" set to 2. Then the default model for evaporation that handle the alpha "cluster" release by the excited nucleus after pre-equilibrium stage is the ABLA model [7]. Nevertheless, this approach with INCL4/ABLA model is suffering from the non-transport of heavy ions. Therefore, the transport mode for the run with the INCL4/ABLA model, is set within "mode n h a" without #. This issue is overcome by a second run with previous set of parameters, i.e., default model, to simulate this missing contribution of the lineal energy distribution.

IV – Results and discussion.

In what follows, the first part is devoted to a comparison of the 13.9 MeV lineal energy spectrum between experience and simulations with successively default and INCL4/ABLA models. The 13.9 MeV energy provides the advantage to be above the capture threshold and implies alpha release from the compound nucleus. In a second part, simulated kerma factor, mean quality factor and ambient dose equivalent with the standard TEPC are compared to ICRU and ICRP standard values for mono-energetic neutrons from 100 keV to 19 MeV, AmBe and ^{252}Cf sources.

IV.1 – Benchmark for 13.9 MeV neutrons

In the experiment performed by Menzel & al. [3], the detector was irradiated by monoenergetic neutrons produced by the fusion reaction $^{3}H(d,n)\,^{4}He$ from a solid-state tritium targets bombarded with deuterons of appropriate energy from a Van de Graaff accelerator. The center-to center separation distance between source and detector is 30 cm. Figure 3-a) shows the microdosimetric spectra derived after pulse processing for 13.9 MeV neutrons. The spectra are plotted with y-axis expressed as $yd(y)$ and x-axis as y in keV.µm^{-1}. As usual, $yd(y)$ spectra are normalized to have unity integral. However, if the y-axis is expressed as $yd(y)\,K_n/\Phi$ – as in the original paper of Menzel & al. - the total area under the curve provides the kerma factor K/Φ related to the entire charge Q from the integration of the $qn(q)$ distribution (see section II). The figure 3-a) also shows spectra simulated with default model and with INCL4/ABLA model for a standard TEPC and 13.9 MeV neutrons. When considering the experimental distribution as reference (blue curve), the prominent peak, centered at about 10 keV.µm^{-1} is related to recoil proton from the predominant interaction of elastic scattering from hydrogen and for a slight part from (n,p) capture reactions. This peak extends to the unbreakable proton edge at about 150 keV.µm^{-1} (beyond 100 keV stopping power is responsible for an energy imparted in the inner gaz less than or equal to 100 keV, i.e. for $y = 150\ keV.\mu m^{-1}$). The second peak, at about 300 keV.µm^{-1}, is related to alpha release and extends to the α-edge at about 380 keV.µm^{-1}. The weak bump on the very right end of the curve, up to 2000 keV.µm^{-1} concerns recoil heavy ions: C, N and O. Regarding the set of curves, one may infer an overall good overlapping between experimental and simulated spectra with INCL4/ABLA model unlike the default model that reveals an alpha peak largely underestimated compared to the reported experimental spectrum. The decrease of the maximum-peak value for protons, comparing default and INCL4/ABLA models, stems for the emergence of an largest alpha bump while the whole distribution is normalized to unity. The figure 3-b) details plots contributions of secondary protons, alpha and heavy ions for same energy with INCL4/ABLA model, the blue contribution reveals the alpha bump through the use of anticoincidence pulse eight feature with the pulse eight tally.

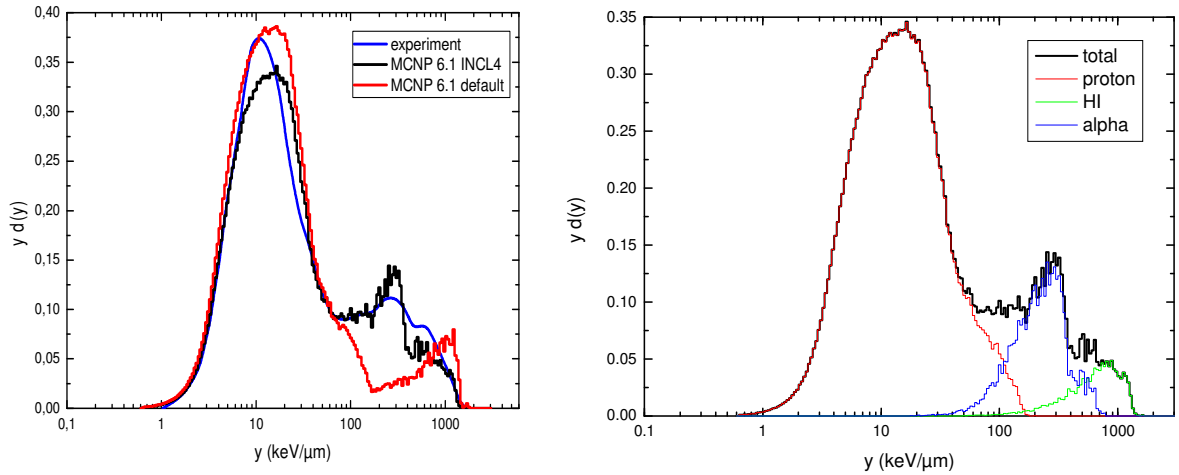

Figure 3 : a) microdosimetric spectra in terms of $yd(y)$ distribution measured by Menzel & al. (blue), simulated with default model (red) and with INCL4/ABLA model (black) for a standard TEPC and 13.9 MeV neutrons b) plots contribution of secondary protons, alpha and heavy ions for same TEPC and energy with INCL4/ABLA model.

With respect to kerma factor evaluation, the expression (eq.1) gives $68.4\ pGy.cm^2$ with the experimental measured intensity $i = dQ/dt = 2.75 \times 10^{-2} pA$ and the neutron fluence rate $\dot{\Phi} = 1.33 \times 10^{5}\ (n) cm^{-2} s^{-1}$ at the reference point of the cavity. A weak difference is found with The ICRU 63 value, $66.5\ pGy.cm^2$, based upon Caswell & al. calculation with equation (2). Simulated results obtained with default and INCL4/ABLA models are respectively: $54.1 \pm 0.1\ pGy.cm^2$

and $69.7 \pm 0.2\ pGy.cm^2$. This Kerma benchmark conclude to a large discrepancy between the default model and experimental/ICRU values while it reveals a quite good agreement with INCL4/ABLA models with both reference values. This conclusion is supported by the analysis of calculated percentage kerma to secondary particle contributions shown in table 1. for which theoretical value is calculated with eq. 2 and cross sections from JEFF-3.1[18] and ENDF/B-VII.0 [19] libraries. This calculation handles the $^{12}C(n,3\alpha)$ reaction channel contribution with $\sigma = 300\ mb$ [20]. Theoretical percentage kerma to secondary particle contributions are consistent with the Meulders & al. values within few percent [21].

Origin	Protons	Alpha	Heavy ions
Theoretical (eq. 2)	78.9	11.4	9.7
Default model	90.3	1.1	8.6
INCL4/ABLA	79.5	15.2	5.3

Table 1 : calculated percentage kerma to secondary particle contributions

This table emphasizes the large underestimation of the alpha release with the default model relative to the INCL4/ABLA model. Nevertheless, the alpha contribution overestimates value found by theoretical evaluation, thereby decreasing the heavy ions percentage.

IV.2 – Overall evaluation for neutron energies from 100 keV up to 19 MeV

Below 100 keV, the "single collision" kerma factor differs significantly from $D^*(10)$ as the energy decreases [22]. The underestimation of $D^*(10)$ by the Kerma factor mainly lies in the importance of multi-scatterings vs. attenuation under the depth of 10 mm inside the ICRU sphere. Consequently, the "single collision" Kerma does not constitute a well-suite estimator of $D^*(10)$ below this energy. That is why the herein Kerma evaluation for mono-energetic neutrons boots from this cut-off energy. The Figures 4 a) and b) display the lineal energy spectra for the energy range of 100 keV to 19 MeV developed with the INCL4/ABLA model.

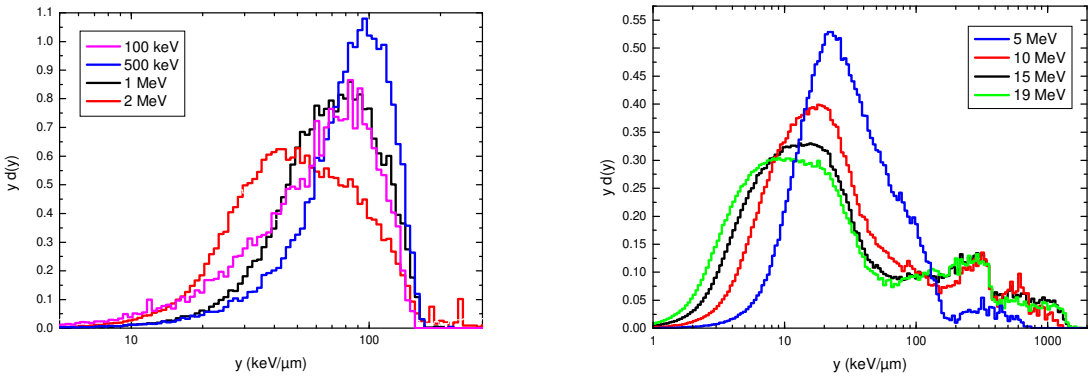

Figure 4 a) Lineal energy spectra from 100 keV to 2 MeV simulated with INCL4/ABLA model b) from 5 MeV to 19 MeV

At all energies, the overall shape of the curves as well as bumps and maximum peak values are consistent with those found in literature [3][4][8][27]. This finding confirms the reliability of MCNP6.1 used for microdosimetric spectra. In table 2, simulated results of the kerma factors, mean frequency energies, mean lineal energies and mean quality factors are presented. The associated uncertainty to the kerma factor based upon (eq.5) is calculated as:

$$\sigma\left(\frac{K}{\Phi}\right) = \frac{1{,}6.\,10^{-10}}{\Phi\rho V}\left[\sum_i (\varepsilon_i\sigma_i)^2\right]^{1/2}$$

With σ_i the statistical uncertainty from MCNP for the lineal energy bin i. The associated uncertainties to mean frequency energy and mean lineal energy based upon (eq. 3 and eq. 4) are :

$$\sigma(\bar{y}_f) = \bar{y}_f\left[\left(\frac{\sqrt{\sum_i(\varepsilon_i\sigma_i)^2}}{\sum_i \varepsilon_i n_i}\right)^2 + \left(\frac{\sqrt{\sum_i \sigma_i^2}}{\sum_i n_i}\right)^2\right]^{1/2} \;;\; \sigma(\bar{y}_D) = \bar{y}_D\left[\left(\frac{\sqrt{\sum_i(\varepsilon_i^2\sigma_i)^2}}{\sum_i \varepsilon_i^2 n_i}\right)^2 + \left(\frac{\sqrt{\sum_i(\varepsilon_i\sigma_i)^2}}{\sum_i \varepsilon_i n_i}\right)^2\right]^{1/2}$$

In the table 2, a synthesis of the benchmark is drawn up with reference values of Kerma factor from ICRU report 63. Table 3 shows the comparison of the mean quality factor $\bar{Q}$ based upon (eq. 5) and the standard quality factor $Q^*(10)$ inside de ICRU sphere [12]. A final comparison concerns the estimator $\hat{H}/\Phi$ versus standard coefficient $H^*(10)/\Phi$ from the ICRP 74 [23].

E (MeV)	$\bar{y}_f$ (keV.µm^{-1})	$\bar{y}_D$ (keV.µm^{-1})	$(K/\Phi)_{MCNP}$ (pGy.cm^2)	$(K/\Phi)_{ICRU}$ (pGy.cm^2)	ΔK
0.1	39.1 ± 0.6	64.4 ± 1.4	6.5 ± 0.1	6.9	-5.25%
0.5	62.8 ± 0.8	83.1 ± 1.2	$16{,}4 \pm 0.2$	16,5	-0,6%
1	55.3 ± 0.5	72.7 ± 0.8	$23{,}4 \pm 0.2$	24,3	-3,7%
2	39.2 ± 0.2	58.5 ± 0.8	30.8 ± 0.1	32	-3,7%
5	20.9 ± 0.1	46.7 ± 0.7	$41{,}7 \pm 0.1$	45,5	-8,3%
10	14.1 ± 0.1	79.2 ± 1.4	58 ± 0.2	58,5	-0,8%
13.9	11.4 ± 0.1	87.7 ± 1.1	$69{,}7 \pm 0.2$	66,5	4,8%
15	10.8 ± 0.1	92.0 ± 1.5	71.7 ± 0.2	67.4	6,4%
19	8.85 ± 0.1	84.2 ± 1.2	$73{,}2 \pm 0.2$	73,3	-0,1%

Table 2 : Kerma factor, mean frequency energy, mean lineal energy calculated upon INCL4/ABLA results and relative deviation on Kerma factor with standard values, for mono-energies from 0.1 to 19 MeV

E (MeV)	$\bar{Q}$ (Sv.Gy^{-1})	$Q^*(10)$ (Sv.Gy^{-1})	ΔQ	$(\hat{H}/\Phi)$ (pSv.cm^2)	$(H^*(10)/\Phi)$ (pSv.cm^2)	ΔH
0.1	18.4	15	22.7%	120	88	35.9%
0,5	22,8	20,1	13,4%	374	322	16,1%
1	20,4	17,8	14,8%	477	416	14,8%
2	16,2	13,5	20,0%	499	420	18,8%
5	10,7	8,7	22,3%	446	405	10,2%
10	9,1	6,9	31,9%	528	440	20,0%
13,9	8,8	7,1	23,9%	611	520	17,4%
15	8,6	7,2	18,9%	614	540	13,7%
19	8,2	7,3	12,7%	598	580	3,1%

Table 3 : Mean quality factor and fluence-to-ambient dose equivalent coefficient evaluation calculated upon INCL4/ABLAABLA results and relative deviations with standards values, for mono-energies from 0.1 to 19 MeV

Table 2 reveals a relative deviation within 8.5% with a mean value of 4.4% which may be regarded as a satisfactory agreement with standards values and validate the proposed MCNP approach for such calculation. Nevertheless, table 3 shows a relative deviation within 36% with a mean value of 16.6% for the evaluation of fluence-to-ambient dose equivalent coefficients because of the poor evaluation of $Q^*(10)$ with the mean quality factor $\bar{Q}$ based upon calculation with the whole y_i (see eq. 5). The same conclusion can be drawn with respect of the other calculation method for $\bar{Q}$ proposed by Kellerer & al. [31] that lead to relative deviation within the same order of magnitude. The underlying causes of this discrepancy probably stem from differences in energy spectrum and multi-scattering undergone at the depth of 10 mm within the ICRU sphere versus in the methane-TE gaz. In the gaz, the mean quality factor $\bar{Q}$ is not sufficiently representative whatever the calculation method used. These finding on the systematic deviation between $H^*(10)$

and the estimator $K.\bar{Q}$, for same energy range, is a recurrent issue highlighted in literature Moslehi & Raisaliand [32] not attributable to the new proposed approach.

IV.3 – Evaluation for AmBe and ^{252}Cf sources

Figure 5 shows lineal energy spectra for AmBe and ^{252}Cf point-sources without transport of photons for modelling gamma rays. This omission, for AmBe, results in the lack of the 60 keV gammas that contribute at lineal energies lower than 10 keV.µm^{-1}. For neutrons, the spectra simulated by MCNP are comparable to those of the literature [6], [24]. The slight left shift of the AmBe proton peak relative to that of ^{252}Cf is largely attributable to the difference in the mean energy of flux spectra, respectively 3.27 MeV and 1.9 MeV in terms of weighted average over the ambient dose equivalent spectrum.

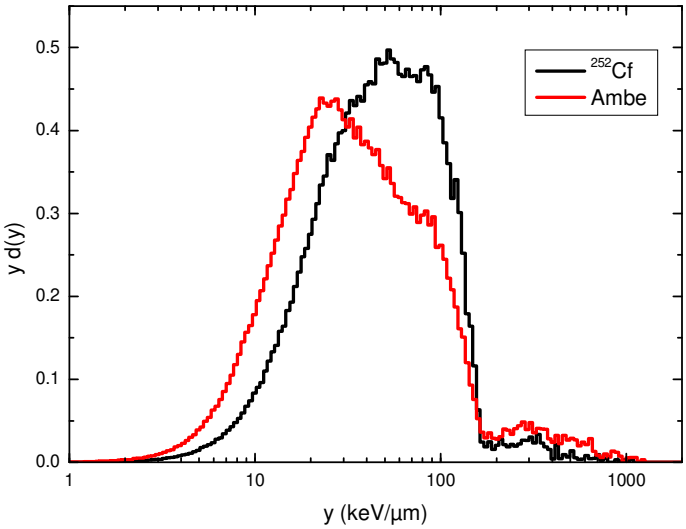

Figure 5 : lineal energy spectra from 100 keV to 5 MeV simulated with INCL4/ABLA model

Table 4 and 5 provides same simulated results and deviations than above for both sources.

source	$\bar{y}_f$ (keV.µm^{-1})	$\bar{y}_D$ (keV.µm^{-1})	$(K/\Phi)_{MCNP}$ (pGy.cm^2)	$(K/\Phi)_{ICRU}$ (pGy.cm^2)	ΔK
AmBe	22.2 ± 0.1	58.3 ± 0.9	37.0 ± 0.1	39.4	-6.1%
^{252}Cf	31.5 ± 0.1	60.4 ± 0.6	$29{,}2 \pm 0.1$	29,7	1,58%

Table 4 :Kerma factor, mean frequency energy, mean lineal energy calculated upon INCL4/ABLA results and relative deviation on Kerma factor with standard values, for AmBe and ^{252}Cf

source	$\bar{Q}$ (Sv.Gy^{-1})	$Q^*(10)$ (Sv.Gy^{-1})	ΔQ	$(\hat{H}/\Phi)$ (pSv.cm^2)	$(H^*(10)/\Phi)$ (pSv.cm^2)	ΔH
AmBe	12.2	10.9	12,3%	451	391	15,4%
^{252}Cf	15.3	14.0	9,3%	477	447	16,2%

Table 5 : mean quality factor and fluence-to-ambient dose equivalent coefficient evaluation calculated upon INCL4/ABLA results and relative deviations with standards values, for AmBe and ^{252}Cf

Although kerma measurement with standard TEPC is not relevant for low-energy neutrons, particularly for the case of AmBe spectrum, discrepancies do not exceed 7% for overall Kerma. With respect to the evaluation of fluence-to-ambient dose equivalent coefficient, results suffer same shortcoming as mono-energy evaluation, meaning an overestimation within 17%. Figure 6 displays a synthesis of Kerma calculation with the INCL4/ABLA evaluation, relative to ICRU report 63 standard values presented as a curve-fitting and measurement results from Menzel & al. for 13.9 MeV and 19 MeV neutrons.

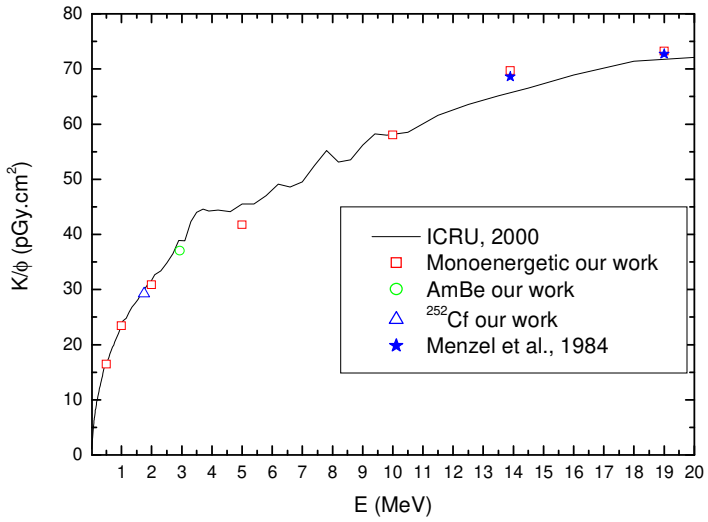

Figure 6 : synthesis of Kerma factor calculation with INCL4/ABLA model realative to measurement values of Menzel & al. for 13.9 et 19 MeV neutrons and standard values from ICRU report 63 [11]

One may infer that the MCNP results closely match to the ICRU reference curve for Kerma factor, whether for mono-energies and spectra. This finding henceforth offers the prospect to simulate microdosimetric spectra with TEPC, for energies upper than a hundred keV like GEANT4 or FLUKA codes.

V – Conclusion

So far, previous studies have emphasized the reliability of Monte-Carlo transport codes as GEANT4 or FLUKA to develop lineal energy spectra consistent with experimental ones for several TEPC and furthermore evaluate the single collision Kerma for neutrons. Nevertheless, no investigations led to same conclusion for MCNP6.1. The main reason of the unreliability of MCNP6.1 was mainly attributable to the underestimation of the alpha release by capture reaction resulting in a unrepresentative weak bump in lineal energy spectra and consequently a poor kerma evaluation for energy region over capture threshold (roughly above 4 MeV). This paper highlights the improvement provided by the implementation of the intranuclear cascade model INCL4/ABLA in the physics parameters to simulate the alpha release and enhance the heavy ion contribution. This new approach lead to lineal energy spectra similar to those from experiment and a kerma evaluation with a mean relative deviation not exceeding 5% of standard values for mono-energy ranging over 100 keV to 19 MeV. This new approach is also relevant for usual neutron sources as AmBe and ^{252}Cf with a maximum deviation of roughly 6%. Nevertheless, major discrepancies remain for evaluation of the quality factor at the depth of 10 mm inside de ICRU sphere, with a mean relative deviation of 17%. As regards the prospects, satisfactory results on lineal energy spectra and kerma evaluation henceforth offers the possibility to simulate microdosimetric spectra and determine neutron kerma for energies upper than a hundred keV with TEPC. For instance, this new approach for simulation could be extended to other TEPC like THGEM-based microdosimeter currently under development. In addition, further investigations could be carried out on others wall materials with different carbon content, e.g., ICRU composition.

Reference

[1] Rossi H H 1968 Radiation Dosimetry vol. 1 (New York: Academic Press) pp43-85

[2] Y. Nakane, Y. Sakamoto « Measurement of absorbed dose distributions in a plastic phantom irradiated by 40- and 65-MeV quasi-monoenergetic neutrons » Nuclear Instruments and Methods in Physics Research A 459 (2001) 552}564

[3] H G Menzel, G Buhler, H Schuhmacher H Muth, G Dietze and S Guldbakke, "Ionisation distributions and A-150 plastic kerma for neutrons between 13.9 and 19.0 MeV measured with a low pressure proportional counter" Phys. Med. Biol. 29 1537, 1984

[4] T. Nunomiya, E. Kim, T. Kurosawa, S. Taniguchi, T. Nakamura, Y. Nakane, Y. Sakamoto and S. Tanak, "measurement of lineal-energy distributions for neutrons of 8 keV to 65 Mev by using a tissue-equivalent proportional counter" Radiation Protection Dosimetry Vol. 102, No. 1, pp. 49–59 (2002)

[5] A. Hanu, S.H.Byun, W.V.Prestwich "A Monte Carlo simulation of the microdosimetric response for thick gas electron multiplier" Nuclear Instruments and Methods in Physics Research A 622 (2010) 270–275

[6] A. Moslehi, G. Raisali, M. Lamehi, « Simulation and experimental study of an indigenously designed and constructed THGEM-based microdosimeter for dose-equivalent measurement » Radiation Measurements 86 (2016).

[7] Pelowitz D. B. (ed.) (2013). MCNP6 USER'S MANUAL Version 1.0 Manual Rev. 0 Editor: LA-CP-13-00634, Rev. 0.

[8] F. Ali, A. J.Waker and E. J.Waller "Intercomparison of monte carlo radiation transportcodes to model tepc response in low-energy neutron and gamma-ray fields" Radiation Protection Dosimetry (2014), Vol. 161, No. 1–4, pp. 257–260

[9] A. Boudard, J. Cugnon, S. Leray and C. Volant, "Intranuclear cascade model for a comprehensive description of spallation reaction data" Physical Review C 66, 044615 (2002).

[10] R. S. Caswell, J. J. Coyne and M. L. Randolph, "Kerma Factors of Elements and Compounds for Neutron Energies Below 30 MeV" " Int. J. Appl. Radiat. Isot. Vol. 33, 1227 to 1262. 1982

[11] ICRU Report 63. Nuclear Data for Neutron and Proton Radiotherapy and for Radiation Protection BETHESDA (2000)

[12] Leuthold G. Mares V. Schaube H. (1992) calculation of the neutron ambient dose equivalent on the basis of the ICRP revised quality factor. Radiation Protection Dosimetry Vol. 40 n°2 pp 77-84

[13] ICRU report 36, Microdosimetry Washington, DC (1983)

[14] J. J. Ritts, M. Solomito & P. N. Stevens "Calculation of Neutron Fluence-to-Kerma Factors for the Human Body Nuclear Applications and Technology, 7:1, 89-99, 1969

[15] McConn Jr et al.] RJ McConn Jr, CJ Gesh, RT Pagh, RA Rucker, RG Williams III Compendium of Material Composition Data for Radiation Transport Modeling PNNL-15870 Rev.1

[16] F. Ali, "Design and Characterization of Next-Generation Tissue Equivalent Proportional Counters for use in Low Energy Neutron" Fields Thesis Faculty of Energy Systems and Nuclear Science University of Ontario Institute of Technology, 2014

[17] A.J. Koning and D. Rochman, "Modern Nuclear Data Evaluation With The TALYS Code System", Nuclear Data Sheets 113 (2012) 2841

[18] M.A. Kellett, O. Bersillon, R.W. Mills, The JEFF3.1/3.1.1 radioactive decay data and fission yields sublibraries, JEFF report 20, (NEA/OECD, Paris 2009).

[19] M.B. Chadwick et al., ENDF/B-VII.0: Next Generation Evaluated Nuclear Data Library for Nuclear Science and Technology, Nuclear Data Sheets 107, 2931 (2006).

[20] Antolković B., Šlaus I., Plenković D., Macq P., Meulders J.P. (1983) Study of the Reaction 12C(n,3 α)n from Threshold to En=35 MeV. In: Böckhoff K.H. (eds) Nuclear Data for Science and Technology. Springer, Dordrecht

[21] J.P. Meulders, S. Benck, and I. Slypen,"Experimental kerma coefficients of biologically important materials at neutron energies below 75 MeV", Med. Phys. 27 (11), November 2000

[22] R. Antoni, L. Bourgois, Ionizing Radiation Interaction in Tissues: Kerma and the Absorbed Dose in "Applied Physics of External Radiation Exposure Dosimetry and Radiation Protection" Springer (2017) https://doi.org/10.1007/978-3-319-48660-4_2

[23] ICRP, 1996. Conversion Coefficients for use in Radiological Protection against External Radiation. ICRP Publication 74.

[24] G.C. Taylor, N.P. Hawkes, A. Shippen, "Accurate simulations of TEPC neutron spectra using Geant4", Radiation Physics and Chemistry 116 (2015) 186–188

[25] ICRU Report 40 the Quality factor in Radiation Protection, ICRU Report 40 (1986)

[26] Antoni R, Bourgois L Evaluation of the new electron-transport algorithm in MCNP6.1 for the simulation of dose point kernel in water Nuclear Inst. and Methods in Physics Research, B 412 (2017) 102–108

[27] Stark M S, Waker A J Hunt J B The determination of fluence to dose equivalent conversion factors for americium-Beryllium and californium sources from microdosimetric measurements Radiation Protection Dosimetry Vol. 18 n° 3 pp 141-146 (1987)

[28] J. J. Gaimard and K. H. Schmidt, "A reexamination of the abrasion ablation model for the description of the nuclear fragmentation reaction," Nucl. Phys. A 531, pp. 709–745 (1991).

[29] A. R. Junghans, M. de Jong, H.-G. Clerc, A. V. Ignatyuk, G. A. Kudyaev, and K.-H. Schmidt, "Projectile-Fragment Yields as a Probe for the Collective Enhancement in the Nuclear Level Density," Nucl. Phys. A 629, 635–655 (1998).

[30] A. Seldak, "some properties of the microdosimetric quality factor" Radiation Protection Dosimetry Vol. 38, No. 4, pp. 279-285 (1991)

[31] Kellerer, A.M., Hahn, K., 1988. Considerations on a revision of the quality factor. Radiat. Res. 114, 480-488.

[32] Amir Moslehi, Gholamreza Raisali, 2018 Simulated response of a multi-element thick gas electron multiplier-based microdosimeter to high energy neutrons Applied Radiation and Isotopes 137 (2018) 236–240